Eur. Phys. J. C 29, 171–179 (2003)
Digital Object Identifier (DOI) 10.1140/epjc/s2003-01232-3

THE EUROPEAN PHYSICAL JOURNAL C

Double-spin asymmetries in the cross section of ρ^0 and ϕ production at intermediate energies

The HERMES Collaboration

A. Airapetian[32], N. Akopov[32], Z. Akopov[32], M. Amarian[6,32], V.V. Ammosov[24], A. Andrus[15], E.C. Aschenauer[6], W. Augustyniak[31], R. Avakian[32], A. Avetissian[32], E. Avetissian[10], P. Bailey[15], V. Baturin[23], C. Baumgarten[21], M. Beckmann[5], S. Belostotski[23], S. Bernreuther[29], N. Bianchi[10], H.P. Blok[22,30], H. Böttcher[6], A. Borissov[19], M. Bouwhuis[15], J. Brack[4], A. Brüll[18], V. Bryzgalov[24], G.P. Capitani[10], H.C. Chiang[15], G. Ciullo[9], M. Contalbrigo[9], G.R. Court[16], P.F. Dalpiaz[9], R. De Leo[3], L. De Nardo[1], E. De Sanctis[10], E. Devitsin[20], P. Di Nezza[10], M. Düren[13], M. Ehrenfried[8], A. Elalaoui-Moulay[2], G. Elbakian[32], F. Ellinghaus[6], U. Elschenbroich[11], J. Ely[4], R. Fabbri[9], A. Fantoni[10], A. Fechtchenko[7], L. Felawka[28], B. Fox[4], J. Franz[11], S. Frullani[26], Y. Gärber[8], G. Gapienko[24], V. Gapienko[24], F. Garibaldi[26], E. Garutti[22], D. Gaskell[4], G. Gavrilov[23], V. Gharibyan[32], G. Graw[21], O. Grebeniouk[23], L.G. Greeniaus[1,28], W. Haeberli[17], K. Hafidi[2], M. Hartig[28], D. Hasch[10], D. Heesbeen[22], M. Henoch[8], R. Hertenberger[21], W.H.A. Hesselink[22,30], A. Hillenbrand[8], Y. Holler[5], B. Hommez[12], G. Iarygin[7], A. Ivanilov[24], A. Izotov[23], H.E. Jackson[2], A. Jgoun[23], R. Kaiser[14], E. Kinney[4], A. Kisselev[23], K. Königsmann[11], H. Kolster[18], M. Kopytin[23], V. Korotkov[6], V. Kozlov[20], B. Krauss[8], V.G. Krivokhijine[7], L. Lagamba[3], L. Lapikás[22], A. Laziev[22,30], P. Lenisa[9], P. Liebing[6], T. Lindemann[5], K. Lipka[6], W. Lorenzon[19], B. Maiheu[12], N.C.R. Makins[15], B. Marianski[31], H. Marukyan[32], F. Masoli[9], F. Menden[11], V. Mexner[22], N. Meyners[5], O. Mikloukho[23], C.A. Miller[1,28], Y. Miyachi[29], V. Muccifora[10], A. Nagaitsev[7], E. Nappi[3], Y. Naryshkin[23], A. Nass[8], W.-D. Nowak[6], K. Oganessyan[5,10], H. Ohsuga[29], G. Orlandi[26], N. Pickert[8], S. Potashov[20], D.H. Potterveld[2], M. Raithel[8], D. Reggiani[9], P. Reimer[2], A. Reischl[22], A.R. Reolon[10], K. Rith[8], G. Rosner[14], A. Rostomyan[32], L. Rubacek[13], D. Ryckbosch[12], Y. Salomatin[24], I. Sanjiev[2,23], I. Savin[7], C. Scarlett[19], A. Schäfer[25], C. Schill[11], G. Schnell[6], K.P. Schüler[5], A. Schwind[6], R. Seidl[8], B. Seitz[13], R. Shanidze[8], C. Shearer[14], T.-A. Shibata[29], V. Shutov[7], M.C. Simani[22,30], K. Sinram[5], M. Stancari[9], M. Statera[9], E. Steffens[8], J.J.M. Steijger[22], J. Stewart[6], U. Stösslein[4], P. Tait[8], H. Tanaka[29], S. Taroian[32], B. Tchuiko[24], A. Terkulov[20], E. Thomas[10], A. Tkabladze[6], A. Trzcinski[31], M. Tytgat[12], G.M. Urciuoli[26], P. van der Nat[22,30], G. van der Steenhoven[22], R. van de Vyver[12], M.C. Vetterli[27,28], V. Vikhrov[23], M.G. Vincter[1], J. Visser[22], C. Vogel[8], M. Vogt[8], J. Volmer[6], C. Weiskopf[8], J. Wendland[27,28], J. Wilbert[8], T. Wise[17], S. Yen[28], S. Yoneyama[29], B. Zihlmann[22,30], H. Zohrabian[32], P. Zupranski[31]

[1] Department of Physics, University of Alberta, Edmonton, Alberta T6G 2J1, Canada
[2] Physics Division, Argonne National Laboratory, Argonne, Illinois 60439-4843, USA
[3] Istituto Nazionale di Fisica Nucleare, Sezione di Bari, 70124 Bari, Italy
[4] Nuclear Physics Laboratory, University of Colorado, Boulder, Colorado 80309-0446, USA
[5] DESY, Deutsches Elektronen-Synchrotron, 22603 Hamburg, Germany
[6] DESY Zeuthen, 15738 Zeuthen, Germany
[7] Joint Institute for Nuclear Research, 141980 Dubna, Russia
[8] Physikalisches Institut, Universität Erlangen-Nürnberg, 91058 Erlangen, Germany
[9] Istituto Nazionale di Fisica Nucleare, Sezione di Ferrara and Dipartimento di Fisica, Università di Ferrara, 44100 Ferrara, Italy
[10] Istituto Nazionale di Fisica Nucleare, Laboratori Nazionali di Frascati, 00044 Frascati, Italy
[11] Fakultät für Physik, Universität Freiburg, 79104 Freiburg, Germany
[12] Department of Subatomic and Radiation Physics, University of Gent, 9000 Gent, Belgium
[13] Physikalisches Institut, Universität Gießen, 35392 Gießen, Germany
[14] Department of Physics and Astronomy, University of Glasgow, Glasgow G128 QQ, United Kingdom
[15] Department of Physics, University of Illinois, Urbana, Illinois 61801, USA
[16] Physics Department, University of Liverpool, Liverpool L69 7ZE, United Kingdom
[17] Department of Physics, University of Wisconsin-Madison, Madison, Wisconsin 53706, USA
[18] Laboratory for Nuclear Science, Massachusetts Institute of Technology, Cambridge, Massachusetts 02139, USA
[19] Randall Laboratory of Physics, University of Michigan, Ann Arbor, Michigan 48109-1120, USA
[20] Lebedev Physical Institute, 117924 Moscow, Russia
[21] Sektion Physik, Universität München, 85748 Garching, Germany
[22] Nationaal Instituut voor Kernfysica en Hoge-Energiefysica (NIKHEF), 1009 DB Amsterdam, The Netherlands
[23] Petersburg Nuclear Physics Institute, St. Petersburg, Gatchina, 188350 Russia

[24] Institute for High Energy Physics, Protvino, Moscow oblast, 142284 Russia
[25] Institut für Theoretische Physik, Universität Regensburg, 93040 Regensburg, Germany
[26] Istituto Nazionale di Fisica Nucleare, Sezione Roma 1, Gruppo Sanità and Physics Laboratory, Istituto Superiore di Sanità, 00161 Roma, Italy
[27] Department of Physics, Simon Fraser University, Burnaby, British Columbia V5A 1S6, Canada
[28] TRIUMF, Vancouver, British Columbia V6T 2A3, Canada
[29] Department of Physics, Tokyo Institute of Technology, Tokyo 152, Japan
[30] Department of Physics and Astronomy, Vrije Universiteit, 1081 HV Amsterdam, The Netherlands
[31] Andrzej Soltan Institute for Nuclear Studies, 00-689 Warsaw, Poland
[32] Yerevan Physics Institute, 375036 Yerevan, Armenia

Received: 11 February 2003 /
Published online: 11 June 2003 –

Abstract. Double-spin asymmetries in the cross section of electroproduction of ρ^0 and ϕ mesons on the proton and deuteron are measured at the HERMES experiment. The photoabsorption asymmetry in exclusive ρ^0 electroproduction on the proton exhibits a positive tendency. This is consistent with theoretical predictions that the exchange of an object with unnatural parity contributes to exclusive ρ^0 electroproduction by transverse photons. The photoabsorption asymmetry on the deuteron is found to be consistent with zero. Double-spin asymmetries in ρ^0 and ϕ meson electroproduction by quasi-real photons were also found to be consistent with zero; the asymmetry in the case of the ϕ meson is compatible with a theoretical prediction which involves $s\bar{s}$ knockout from the nucleon.

1 Introduction

Traditionally, diffractive vector-meson production in lepton-nucleon interactions is described as a fluctuation of the virtual photon into a quark-antiquark pair that subsequently forms a vector meson by scattering off the nucleon. For virtual photons with small negative four-momentum squared $Q^2 < 0.5\,\mathrm{GeV}^2$, the formation of the $q\bar{q}$ state is usually described in the framework of Vector Meson Dominance (VMD) [1], while at higher Q^2 it is assumed to follow the scheme of Generalised Vector Meson Dominance (GVMD) [1,2]. In terms of Regge phenomenology [3], the interaction of the virtual vector state with the nucleon can be explained as an exchange of an intermediate object (Reggeon or Pomeron) in the t-channel of the reaction. For various vector mesons, different objects may be exchanged at different values of the invariant mass W of the photon-nucleon system. In principle both Reggeon and Pomeron exchange can contribute to ρ^0 production, while in the case of ϕ production Reggeon-exchange amplitudes are expected to be strongly suppressed [4].

In the Q^2 range covered by the HERMES experiment both longitudinal and transverse photons contribute to vector meson electroproduction [5–7]. For longitudinal photons information about the exchanged object can be extracted through cross-section measurements [8]. For transverse photons this information is accessible through measurements of a double-spin asymmetry that arises in the cross section and is sensitive to the parity[1] of the exchanged object. No asymmetry can arise for longitudinal photons because their helicity is zero.

In general, the photoabsorption asymmetry A_1 describing the spin dependence of the interaction between a transverse photon and a longitudinally polarised nucleon is defined as

$$A_1 = \frac{\sigma_{1/2} - \sigma_{3/2}}{\sigma_{1/2} + \sigma_{3/2}} \,. \tag{1}$$

Here $\sigma_{1/2\ (3/2)}$ stands for the transverse photoabsorption cross section where the subscript denotes the total helicity of the photon-nucleon system. This asymmetry can be expressed in terms of the helicity amplitudes $T^{\lambda_{N'}\lambda_V}_{\lambda_N\lambda_\gamma}$, each of which receives contributions of both natural ($P = (-1)^J$) and unnatural ($P = -(-1)^J$) parities. Here J denotes the total angular momentum of the exchanged particle and λ_γ, λ_V and λ_N ($\lambda_{N'}$) indicate the helicity of the photon, vector meson and nucleon before (after) the interaction, respectively. In the approach of [9], the asymmetry A_1 arises from the interference between the parts of the transverse helicity amplitude T^{11}_{11} with natural and unnatural parities. While a measurable asymmetry can arise even from a tiny contribution of the unnatural parity component, the latter may remain unmeasurable in the total cross section. A significant unnatural-parity contribution indicates the exchange of a di-quark or Reggeon. No asymmetry can be expected in the case of Pomeron exchange, since the Pomeron has natural parity.

The photoabsorption asymmetries presented in this paper are extracted with the aim of studying the mechanism of ρ^0 and ϕ production from transverse photons in the kinematic region covered by the HERMES experiment. Double-spin asymmetries for the production of ρ^0 and ϕ mesons in lepton-nucleon scattering are presented, based on data obtained with a longitudinally polarised electron (positron) beam and longitudinally polarised hydrogen and deuterium targets. Indication of a positive double-spin asymmetry in exclusive ρ^0 meson electroproduction on the proton was reported previously in [10]. This asymmetry is here re-evaluated using an improved data set

[1] In principle, the parity of the object exchanged in vector-meson production can be also extracted from the full set of spin density matrix elements [6,7]

and a new parameterisation of R, the ratio of longitudinal to transverse photoabsorption cross sections.

2 Experiment

The HERMES experiment uses a target of polarised or unpolarised gas internal to the 27.5 GeV electron (positron) beam of the HERA storage ring at DESY. In 1996-1997 (1998-2000) the polarised target was operated with atomic hydrogen (deuterium). The lepton beam is transversely self-polarised by the emission of synchrotron radiation [11]. The longitudinal polarisation at the interaction point is obtained by spin rotators located upstream and downstream of the experiment. The beam polarisation is continuously measured by two Compton polarimeters [12,13]. The average beam polarisation for the proton (deuteron) data set was 0.55 (0.55) with a fractional systematic uncertainty of 3.4 (2.0)%.

The target [14] was fed by an atomic beam source, whose principle of operation is based on Stern-Gerlach separation in conjunction with hyperfine transition units. The average value of the target polarisation for the proton (deuteron) data set was 0.85 (0.85) with a fractional systematic uncertainty of 3.8 (3.5)%.

The HERMES spectrometer is described in detail in [15]. Its angular acceptance in the laboratory frame spans the range $40 < |\theta_y| < 140$ mrad and $|\theta_x| < 170$ mrad, where θ_x and θ_y are the projections of the polar scattering angle into the horizontal and vertical planes. The tracking system has a momentum resolution of about 1.5%. The angular resolution is about 1 mrad. Particle identification is accomplished by a lead-glass calorimeter [16], a preshower and a transition-radiation detector. Until 1998 the particle identification system was complemented by a gas threshold Čerenkov counter, which was then replaced by a dual-radiator ring-imaging Čerenkov detector (RICH), described in detail in [17]. Combining the responses of these detectors in a likelihood method leads to an average electron (positron) identification efficiency of 98% with a hadron contamination less than 1%.

3 Data analysis

3.1 Kinematics

At HERMES, a ρ^0 or ϕ meson is observed through its decay into two pions or kaons, respectively. The kinematics of vector-meson production in lepton-nucleon scattering is described by Q^2, W, the energy ν of the virtual photon in the target rest frame and the four-momentum transfer to the target $-t' = -(t - t_0)$, t_0 being the minimum longitudinal momentum transfer. The "exclusivity" variable $\Delta E = \frac{M_X^2 - M_N^2}{2M_N}$ connects the mass of the target nucleon M_N with the mass of the undetected hadronic system M_X. Also in case of the deuteron all kinematic variables were calculated using the mass of the proton. The Bjørken scaling variable is defined as $x = Q^2/2\nu M_N$.

Two experimental topologies of vector-meson electroproduction at HERMES are considered in the following. The first one is denoted as *exclusive electroproduction*. Here the scattered lepton is detected in the spectrometer acceptance together with the meson decay products. The kinematics of the undetected recoiling nucleon can be reconstructed using those of the meson decay products and of the scattered lepton. The exclusivity of the reaction is enforced by the requirement $\Delta E \approx 0$. At HERMES it results in the following average values: $\langle Q^2 \rangle$=1.8 GeV^2, $\langle W \rangle$=4.9 GeV, $\langle x \rangle$=0.07 and $\langle -t' \rangle$=0.15 GeV^2.

The second topology is *electroproduction by quasi-real photons*. At low values of Q^2 the scattered lepton remains undetected in or close to the beam pipe and the event kinematics cannot be fully determined from the data. The variable ΔE cannot be reliably calculated and hence exclusivity cannot be enforced for events of this topology. Due to the Q^2 dependence of the cross section, low-Q^2 events dominate those where the lepton is undetectable. The average values of Q^2 and x for these events have been determined from Monte Carlo data, generated with the PYTHIA event generator[2] version 6.1 [18] tuned for the kinematics of HERMES. The photon structure was defined according to [19]. Candidate events for ρ^0 (ϕ) meson electroproduction by quasi-real photons were selected requiring two accepted tracks belonging to oppositely charged pions (kaons) having a ρ^0 (ϕ) as a parent particle. The average values of Q^2 and x for these Monte Carlo events were calculated from the kinematics of the scattered positron that escaped the detector acceptance, resulting in $\langle Q^2 \rangle$=0.13 (0.12) GeV^2, $\langle W \rangle$=4.4 (4.2) GeV and $\langle x \rangle$=0.004 (0.006).

3.2 Event selection

The present analysis [20] of double-spin asymmetries in ρ^0 and ϕ meson production is based upon data collected in 1996-2000, using longitudinally polarised hydrogen and deuterium targets. Candidates for exclusive ρ^0 meson (ϕ meson) electroproduction were selected requiring exactly 3 tracks in the detector acceptance, corresponding to the scattered lepton plus two oppositely charged pions (kaons). The vector-meson mass region was defined by the invariant mass constraint $0.6 < M_{\pi\pi} < 0.9$ GeV ($1.01 < M_{KK} < 1.03$ GeV). Cuts were applied on the exclusivity parameter $\Delta E < 0.6$ GeV ($\Delta E < 1.0$ GeV) and the momentum transfer to the target $-t' < 0.4$ GeV^2 ($-t' < 0.6$ GeV^2). Note that in the case of the deuteron both coherent and incoherent parts of the vector-meson production cross section contribute at $-t' < 0.05$ GeV^2. The fraction of the events originating from coherent scattering is not negligible; the ratio of coherent to incoherent cross sections was measured to be 0.160 ± 0.015.

The photon energy was required to fall within $9 < \nu < 22$ GeV. The lower limit is introduced by the kinematic relationship of ν and ΔE, since at $\nu < 9$ GeV non-exclusive events occur at $\Delta E < 3$ GeV, degrading the

[2] This generator was used for all Monte Carlo studies described in the paper except for the acceptance corrections

separation from the exclusive events. The upper cut ensures a high trigger efficiency. The W-acceptance of the HERMES spectrometer for $\rho^0 \to \pi^+\pi^-$ ($\phi \to K^+K^-$) is sharply reduced both below 4 GeV and above 6 GeV, and eliminates any contribution from the nucleon excitation region to ρ^0 (ϕ) production.

Candidate events for ρ (ϕ) electroproduction by quasi-real photons were selected by requiring two tracks belonging to oppositely charged pions (kaons) in the detector acceptance. The same invariant mass constraints as in the case of exclusive electroproduction were applied.

For part of the data sample collected with the hydrogen target, hadron separation was accomplished with the Čerenkov detector. The capability of this detector to identify pions is limited to the momentum range $p_h > 3.5$ GeV, which leads to losses in statistics. Therefore the information of the Čerenkov detector was used only in the sample of electroproduction by quasi-real photons. In the data collected with the deuterium target, hadron separation with the RICH detector was used. Restrictions on hadron momenta were applied to provide efficient hadron identification [20]: $p_K > 2$ GeV, $p_\pi > 0.5$ GeV.

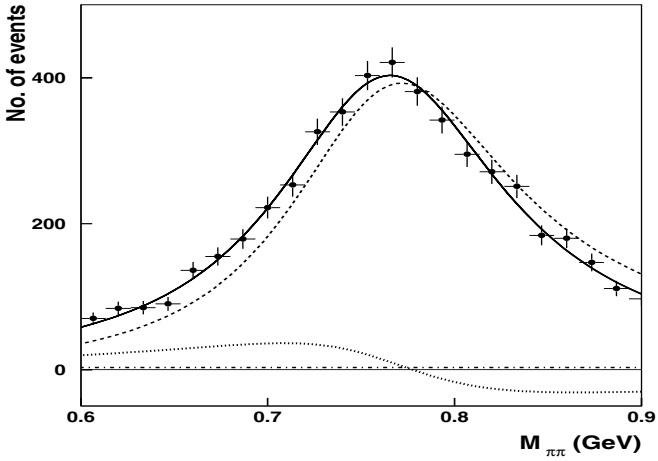

Fig. 1. Subtraction of the non-resonant background. The invariant mass distribution, shown here for exclusive ($\Delta E < 0.6$ GeV) ρ^0 electroproduction on the deuteron, is fitted with a Breit-Wigner shape using the mass skewing model of [21] (solid line). The dashed line indicates the Breit-Wigner function, the dash-dotted line represents the non-resonant background, and the dotted line shows the interference term

3.3 Extraction of double-spin asymmetries

The formalism used here is described in more detail in [10]. The photoabsorption asymmetry A_1 was extracted from the experimental lepton-nucleon asymmetry $A_{||}$ measured using a longitudinally polarised lepton beam and target. These asymmetries are connected as follows:

$$A_1 = \frac{A_{||}}{D} - \eta\sqrt{R}\ . \qquad (2)$$

Here D stands for the fraction of the beam polarisation carried by the photon and $\sqrt{R}$ represents the contribution [10] from the asymmetry A_2 arising from the interference between transverse and longitudinal photons, weighted by the small kinematic factor η, where R is the ratio of longitudinal to transverse cross sections. The definitions of these kinematic variables are given in [10].

In the calculation of asymmetries, background contributions have to be taken into account. Two main types of background can be distinguished: non-resonant background from electroproduction of hadron pairs without formation of an intermediate vector-meson state, and non-exclusive background from vector-meson production with the target nucleon not remaining intact.

The non-resonant background can be subtracted by a fit to the invariant mass distribution, performed separately for each spin configuration of beam and target. The experimental asymmetry $A_{||}^{meas}$ is then calculated as follows:

$$A_{||}^{meas} = \frac{1}{p_B \cdot p_T} \frac{N^{\vec{\Leftarrow}} L^{\vec{\Rightarrow}} - N^{\vec{\Rightarrow}} L^{\vec{\Leftarrow}}}{N^{\vec{\Leftarrow}} L^{\vec{\Rightarrow}} + N^{\vec{\Rightarrow}} L^{\vec{\Leftarrow}}}\ . \qquad (3)$$

Here $N^{\vec{\Rightarrow}(\vec{\Leftarrow})}$ are the numbers of vector mesons produced with parallel (antiparallel) orientation of the nucleon helicity with respect to the lepton helicity. They are determined from the fitting procedure and are corrected here for the relative luminosity $L^{\vec{\Leftarrow}(\vec{\Rightarrow})}$. The polarisations of beam and target are denoted by p_B and p_T, respectively.

The asymmetry $A_{||}^{meas}$ still includes non-exclusive background events, which appear mostly at larger values of the exclusivity parameter ΔE. This type of background is formed mainly by events whose final state contains a product of the fragmentation process in deep inelastic scattering (DIS), e.g. a hadron pair, a vector meson, or other particles decaying into them. It is statistically impractical to fit the invariant mass distribution for each bin in ΔE, in order to subtract non-exclusive background from each spin-dependent yield N. Therefore its contribution is taken into account as a dilution of the experimental asymmetry $A_{||}^{meas}$:

$$A_{||}^{excl} = \frac{1}{1-r} \cdot (A_{||}^{meas} - r A_{||}^{ne})\ . \qquad (4)$$

Note that for electroproduction by quasi-real photons the non-exclusive background can not be subtracted since neither the background asymmetry $A_{||}^{ne}$ nor the fraction r can be determined from the data[3].

3.4 Treatment of backgrounds

In the case of exclusive ρ^0 meson electroproduction, the pion pair invariant mass distribution was fitted with a relativistic p-wave Breit-Wigner function taking into account the skewing of the ρ^0 mass peak using the model of [21] (cf. Fig. 1). The detector acceptance changes very little across the employed range in the invariant mass.

[3] From Monte Carlo data, the fraction of pure exclusive vector-meson electroproduction was obtained as 85%, proton break-up occurs in 12% of the cases and the remaining 3% originate from other processes

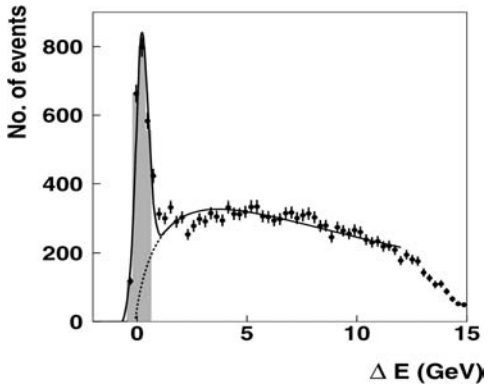

Fig. 2. Subtraction of the non-exclusive background in ρ^0 electroproduction on the proton using a fit method. The ΔE distribution still includes the non-resonant background. The exclusive peak (shaded) is fitted by a Gaussian plus a background function (dashed line, cf. (5)). The solid line represents the sum of the Gaussian and the background

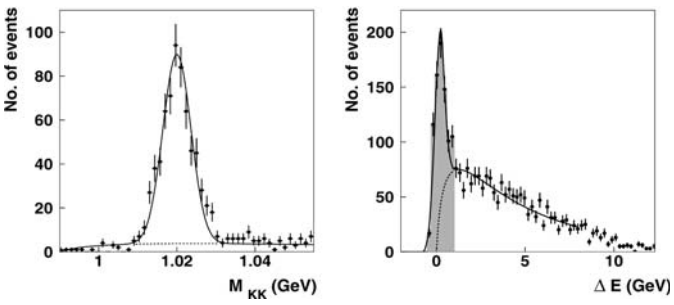

Fig. 3. Subtraction of the non-resonant background (left panel) and of the non-exclusive background (right panel) in ϕ electroproduction on the deuteron. In the left panel the peak is fitted by a Gaussian (solid line) plus a background function (dashed line, cf. (6)). The solid and the dashed lines in the right panel have the same meaning as in Fig. 2. The shaded area indicates the exclusive region

The distribution of the exclusivity parameter ΔE is shown in Fig. 2. The width of the exclusive peak is determined by the detector resolution, resulting in 0.28 (0.38) GeV for the detector configuration in 1996-1997 (1998-2000). Therefore some non-exclusive events appear also under the exclusive peak.

The asymmetry of the non-exclusive background, $A_{||}^{ne}$, was measured to be consistent with zero on both the proton and deuteron in the range $0.6\,\mathrm{GeV} < \Delta E < 5\,\mathrm{GeV}$. It is assumed that the asymmetry of non-exclusive events smeared into the exclusive region is the same. The fraction r of non-exclusive events in the exclusive region $\Delta E < 0.6\,\mathrm{GeV}$ was estimated using a fit of an empirical function to the ΔE spectrum as shown in Fig. 2. A Gaussian distribution was used for the exclusive peak. The background was described by the function

$$f(\Delta E) = a_0 \cdot (\Delta E - a_1) \cdot e^{-a_2\sqrt{\Delta E - a_1}}, \qquad (5)$$

where a_0, a_1 and a_2 are free parameters. This function is intended to account for all types of non-exclusive background like double-dissociative diffraction, DIS and radiative tails. The part of the fitted background distribution falling within the exclusive region $\Delta E < 0.6\,\mathrm{GeV}$ was taken as a measure of the non-exclusive background. The fraction of non-exclusive events was estimated to be $r = 0.13 \pm 0.01 \pm 0.05$ ($0.15 \pm 0.01 \pm 0.07$) in the proton (deuteron) data set. The systematic uncertainty accounts for the range of background shapes that are compatible with the data, and is propagated into the systematic uncertainty of $A_{||}^{excl}$.

The spin-dependent yields in ϕ electroproduction were extracted in a way similar to those for ρ^0 production. Due to limited detector resolution the narrow invariant mass distribution of the kaon pair is widened with respect to its original shape. This effect was studied in [20], using Monte Carlo events which were tracked through the detector taking into account the efficiencies and the resolutions of the detector subsystems. The smeared ϕ resonance peak in the invariant mass distribution of kaon pairs was described by a Gaussian (cf. Fig. 3, left panel). For the background the empirical function

$$f(M_{KK}) = b_0 \cdot (M_{KK} - M_{KK}^{min}) \cdot e^{b_1 \cdot \sqrt{M_{KK} - M_{KK}^{min}}} \qquad (6)$$

was used, where b_0 and b_1 are free parameters and M_{KK}^{min} denotes the threshold of the kaon-pair invariant mass distribution, corresponding to the opening of phase space. The fraction r of non-exclusive events was estimated as described above for the case of ρ^0 production (cf. Fig. 3, right panel) and was found to be $r = 0.28 \pm 0.03 \pm 0.10$ for both targets.

3.5 Acceptance corrections

The data on exclusive electroproduction were corrected for acceptance effects. The corrections were obtained using a multi-dimensional look-up table, calculated from Monte-Carlo data in bins of Q^2, x, $-t'$ and $M_{\pi\pi}$, to account for possible correlations between these variables. The Monte Carlo simulations for the acceptance studies were performed using a generator [22] based on the VMD model. The resulting acceptance correction factors were used as weights for every event depending on its kinematics. The effect of the acceptance correction manifested itself in a shift of at most 8% of the original mean value of the bin center in Q^2 and x at which the asymmetry was evaluated. No shift in t' was observed.

4 Results and interpretation

The photoabsorption asymmetries A_1 for ρ^0 and ϕ electroproduction by quasi-real photons were determined directly from $A_{||}^{meas}$ using (2). In the case of exclusive electroproduction the data were additionally corrected for non-exclusive background using (4), i.e. the photoabsorption asymmetries A_1 were calculated from $A_{||}^{excl}$. The ratio R

Table 1. Photoabsorption asymmetries in vector-meson electroproduction and the numbers of ρ^0 and ϕ mesons used in this analysis. The statistical and systematic uncertainties of the asymmetries are given

	proton	deuteron
	Exclusive electroproduction	
A_1^ρ	0.23 ± 0.14±0.02	-0.040 ± 0.076±0.013
A_1^ϕ	0.20±0.45±0.03	0.17±0.27±0.02
N^ρ	1774	6505
N^ϕ	219	618
	Electroproduction by quasi-real photons	
A_1^ρ	0.0057 ± 0.0093±0.0004	-0.0039 ± 0.0029±0.0003
A_1^ϕ	0.052 ± 0.084±0.003	0.018 ± 0.028±0.001
N^ρ	423×10^3	4013×10^3
N^ϕ	7.6×10^3	57×10^3

Table 2. Measured values of the photoabsorption asymmetry A_1^ρ, shown for various values of each of three kinematic variables while averaging over the other two. Total uncertainties are given

	$\langle D \rangle$	$\langle \eta\sqrt{R} \rangle$	A_1^ρ	
			^{1}H	^{2}H
$\langle x \rangle$				
0.032	0.48	0.029	0.20 ± 0.20	-0.13 ± 0.10
0.057	0.34	0.055	0.28 ± 0.26	0.07 ± 0.14
0.105	0.28	0.098	0.30 ± 0.34	0.09 ± 0.18
$\langle Q^2 \rangle$, GeV^2				
0.84	0.42	0.037	0.17 ± 0.19	-0.03 ± 0.10
1.44	0.34	0.062	0.23 ± 0.26	-0.16 ± 0.14
3.01	0.31	0.099	0.51 ± 0.36	0.19 ± 0.20
$\langle -t' \rangle$, GeV^2				
0.018	0.36	0.059	0.36 ± 0.30	-0.09 ± 0.15
0.065	0.37	0.059	0.16 ± 0.30	-0.05 ± 0.15
0.138	0.36	0.062	0.11 ± 0.31	-0.11 ± 0.16
0.302	0.36	0.063	0.46 ± 0.30	0.17 ± 0.16

was extracted from the elements of the spin-density matrix for vector mesons produced at HERMES [22,23]. The resulting values of A_1 averaged over the kinematics for both the proton and deuteron are listed in Table 1, together with the numbers of ρ^0 and ϕ mesons used in the analysis. For exclusive electroproduction of ρ^0 mesons, the asymmetries A_1 were calculated in several bins of x, Q^2 and t'. In Table 2 the asymmetry values are shown in dependence on each of the three kinematic variables while averaging over the other two. All asymmetries were found to be consistent with zero within experimental uncertainties, possibly apart from the asymmetry in exclusive electroproduction of ρ^0 mesons on the proton. In accordance with an earlier HERMES result [10], the latter was found to have a positive value, 1.7 σ away from zero.

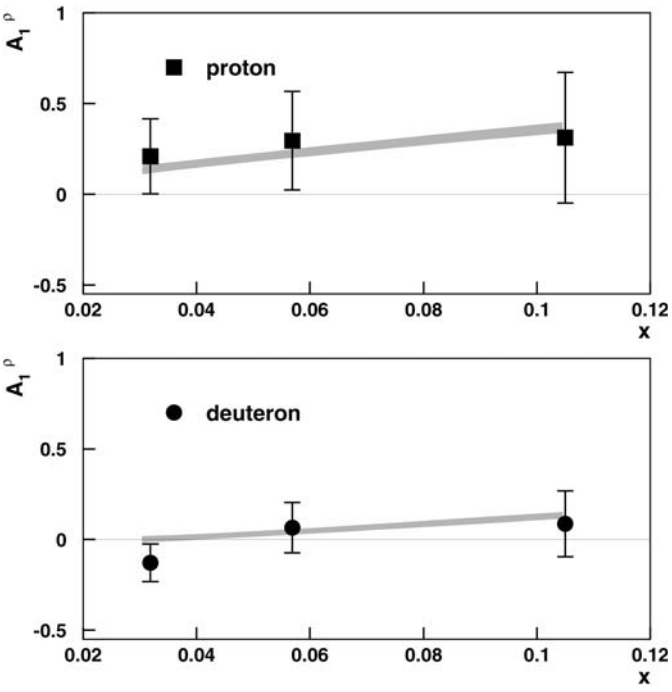

Fig. 4. The x-dependence of the asymmetry A_1^ρ in exclusive ρ^0 meson electroproduction on the proton (top) and deuteron (bottom). The data are compared to the expectations of [9, 10] expressed by (7), as indicated by the shaded bands. The error bars represent the total uncertainties obtained by adding statistical and systematic uncertainties in quadrature

The statistical uncertainties of the extracted numbers of vector mesons per helicity state and of the fraction and asymmetry of the non-resonant background were propagated into the statistical uncertainty of the asymmetry $A_{||}$. The systematic uncertainties from the measurements of $A_{||}^{excl}$, of beam and target polarisation and the uncertainty from the parameterisation of R (cf. (2)) were combined to form the experimental systematic uncertainties to the asymmetry measurements. The systematic uncertainties are found to be considerably smaller than the statistical ones.

The x–dependence of the photoabsorption asymmetry A_1^ρ in exclusive ρ^0 electroproduction is shown in Fig. 4 for both the proton and deuteron. This measurement is compared to the expectation of [9,10] that is based on a relation between the double-spin asymmetries A_1^ρ in exclusive ρ^0 electroproduction and A_1^N in inclusive DIS:

$$A_1^\rho = \frac{2A_1^N}{1 + (A_1^N)^2} \ . \tag{7}$$

Using the HERMES measurements [24] of inclusive DIS asymmetries A_1^N, values for the expected asymmetries A_1^ρ were calculated from (7). The measured asymmetries were found to be consistent with this expectation for both the proton and deuteron.

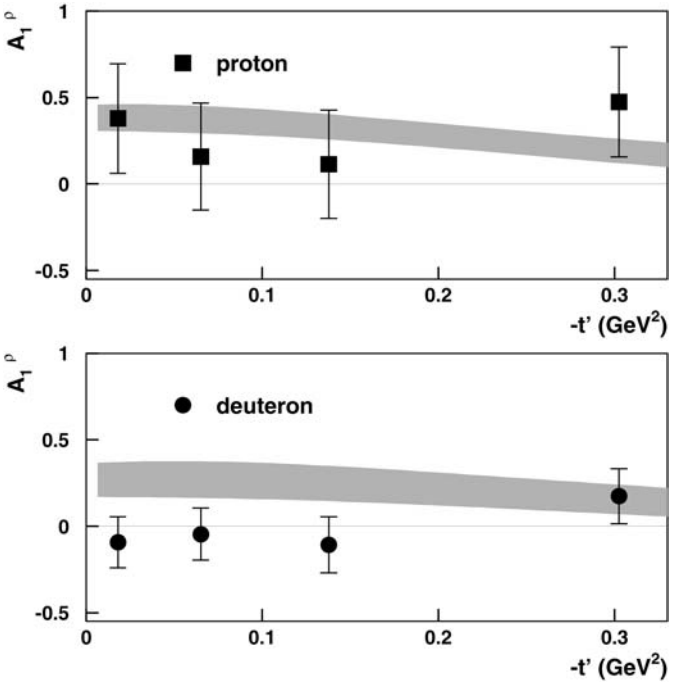

Fig. 5. The $-t'$-dependence of the asymmetry A_1^ρ in exclusive ρ^0 meson electroproduction on the proton (top) and deuteron (bottom). Error bars have the same meaning as in Fig. 4. The shaded areas represent the range allowed for the theoretical predictions of [25]

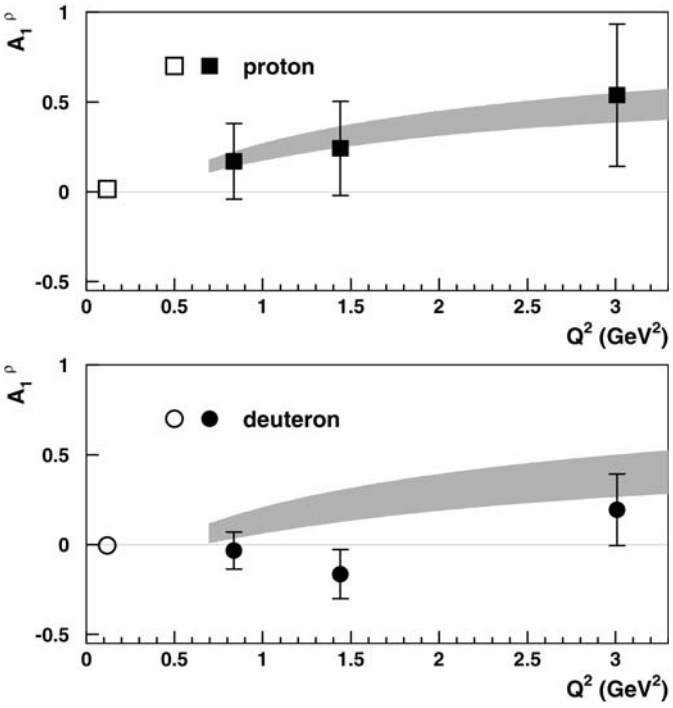

Fig. 6. The Q^2-dependence of the asymmetry A_1^ρ in exclusive electroproduction (closed symbols) and electroproduction by quasi-real photons (open symbols) on the proton (top) and deuteron (bottom). The error bars have the same meaning as in Fig. 4. The uncertainties of the data from electroproduction by quasi-real photons are covered by the symbols. The shaded areas represent the range allowed for the theoretical predictions of [25]

The dependences of A_1^ρ on the momentum transfer $-t'$ and Q^2 are respectively shown in Fig. 5 and Fig. 6 for both the proton and deuteron. They are compared to theoretical predictions calculated recently in the framework of the Regge model [25]. In this approach the parameters of the Reggeons exchanges contributing to ρ^0 meson electroproduction on the nucleon were extracted from fits to the nucleon structure functions g_1^N and F_2^N. These parameters were subsequently used to calculate the ρ^0 electroproduction amplitudes with natural and unnatural parities. Sizeable double-spin asymmetries are predicted for exclusive electroproduction on both proton and deuteron. While the predicted values are consistent with the measured ones on the proton, they are larger in the case of the deuteron.

The double-spin asymmetries in ρ^0 electroproduction by quasi-real photons are also shown in Fig. 6 at the correspondingly low value of Q^2. They are consistent with zero for both the proton and deuteron.

Lepton-nucleon asymmetries in ρ^0 electroproduction by quasi-real photons were measured over a range of values of ρ^0 meson energy and transverse momentum calculated with respect to the beam direction. As can be seen in Fig. 7, no trend was observed in any of these variables. Note that, as was already mentioned above, for electroproduction by quasi-real photons it is not possible to impose the requirement of exclusivity.

Double-spin asymmetries in exclusive ρ^0 meson electroproduction on the proton and deuteron were measured at SMC [26] at $\langle W\rangle$=15 GeV. In this region Pomeron exchange is thought to dominate [2] vector-meson production. In [26] the asymmetries were found to be consistent with zero for both the proton and deuteron in the region $0.01 < Q^2 < 5\,\mathrm{GeV}^2$, and slightly negative at $Q^2 \sim 10\,\mathrm{GeV}^2$. This supports the expectation that Pomeron exchange is dominant at higher energies. In contrast, the tendency for a non-zero double-spin asymmetry found on the proton at HERMES energy suggests a significant contribution of the exchange of Reggeons or di-quark objects to the transverse part of exclusive ρ^0 electroproduction. The asymmetry on the deuteron was measured to be consistent with zero. As unnatural parity exchange need not necessarily produce a non-zero asymmetry on all targets, this does not contradict the conclusion based on that result from the proton target.

In the case of ϕ meson electroproduction, the photoabsorption asymmetries are found to be consistent with zero in both event topologies considered here. A theoretical prediction exists for the case of electroproduction by quasi-real photons. It implies sensitivity of the asymmetry to the strangeness content of the nucleon through interference of $s\bar{s}$ knockout with the diffractive VMD amplitude. In kinematic conditions ($\langle W\rangle = 4.2\,\mathrm{GeV}$, $\langle Q^2\rangle \simeq 0$) similar to those of HERMES, and assuming the strangeness probability for the proton is $P_{s\bar{s}} = 0.01$, the predicted asymmetry [27] at $-t'$=0 ranges between -0.05 and +0.03, while for $-t'$=0.5 GeV^2 the range is -0.06 to +0.15,

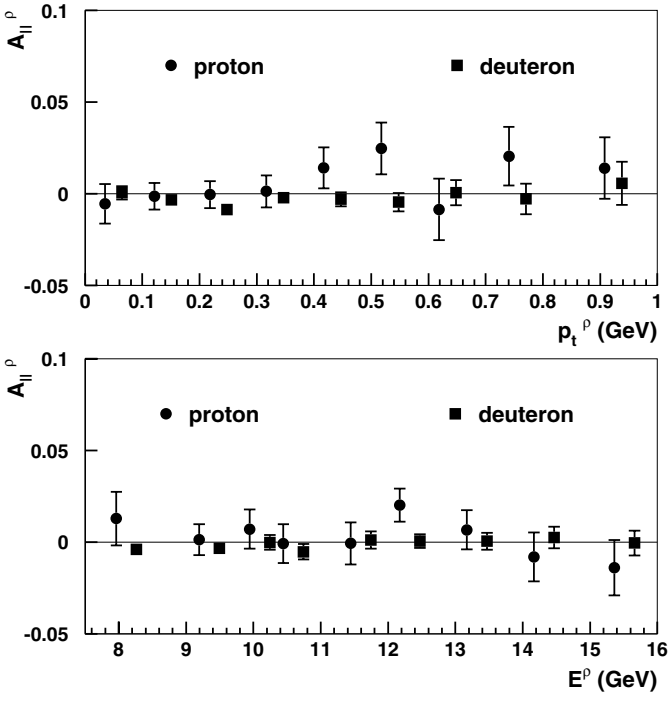

Fig. 7. The dependence on the transverse momentum (top), calculated with respect to the beam direction, and energy of the ρ^0 (bottom) of the asymmetry $A_{||}^{\rho}$ in ρ^0 electroproduction by quasi-real photons on the proton (circles) and deuteron (squares). The proton data are slightly shifted to the left for clearer representation. Error bars have the same meaning as in Fig. 4

depending on the unknown relative phase of the amplitudes. The experimental result is compatible with zero strangeness content, but favours a negative phase $\delta_{s\bar{s}}$ if the strangeness is non-zero as assumed.

5 Summary

Double-spin asymmetries in the cross section of ρ^0 and ϕ electroproduction were measured by scattering longitudinally polarised leptons off longitudinally polarised hydrogen and deuterium targets at HERMES. The analysis was performed for two different event topologies: exclusive electroproduction, and electroproduction by quasi-real photons without the requirement of exclusivity.

The statistically weak evidence of a non-zero double-spin asymmetry in exclusive ρ^0 meson electroproduction on the proton, as reported in [10], is also seen with the improved data set and analysis scheme. This suggests a contribution of unnatural-parity exchange to exclusive ρ^0 electroproduction by transverse photons at HERMES energies. An essentially flat dependence of the proton asymmetry on t' is again observed, consistent with a prediction based on the description of the nucleon structure functions in the framework of the Regge model [25].

The same double-spin asymmetry measured on the deuteron is found to be consistent with zero, which disagrees with the prediction of [25]. The observed difference between the asymmetries measured on the proton and deuteron is consistent, however, with the expectation of [9,10] which relates the asymmetries in ρ^0 production to those in inclusive DIS.

The tendency towards a non-zero asymmetry found in exclusive ρ^0 electroproduction on the proton at HERMES, where quark exchange is expected to contribute substantially [8], can be reconciled with the zero asymmetry measured at the higher energy of the SMC experiment, where Pomeron exchange dominates and therefore no asymmetry in ρ^0 production is expected.

The double-spin asymmetry in ρ^0 electroproduction by quasi-real photons was found to be consistent with zero.

The measured asymmetries for ϕ mesons are consistent with zero within experimental uncertainties, both in exclusive electroproduction and electroproduction by quasi-real photons. This is consistent with the expected dominance of Pomeron exchange in ϕ electroproduction, and, in the case of electroproduction by quasi-real photons, with a theoretical prediction [27] which involves $s\bar{s}$ knockout from the nucleon.

Acknowledgements. We gratefully acknowledge the DESY management for its support and the DESY staff and the staffs of the collaborating institutions. This work was supported by the FWO-Flanders, Belgium; the Natural Sciences and Engineering Research Council of Canada; the INTAS contribution from the European Commission; the European Commission IHP program under contract HPRN-CT-2000-00130; the German Bundesministerium für Bildung und Forschung (BMBF); the Italian Istituto Nazionale di Fisica Nucleare (INFN); Monbusho International Scientific Research Program, JSPS, and Toray Science Foundation of Japan; the Dutch Foundation for Fundamenteel Onderzoek der Materie (FOM); the U.K. Particle Physics and Astronomy Research Council and Engineering and Physical Sciences Research Council; and the U.S. Department of Energy and National Science Foundation.

References

1. T. H. Bauer et al., Rev. Mod. Phys. **50**, No 2, 261 (1978)
2. D. Schildknecht et al., Phys. Lett. B **449**, 328 (1999)
3. A. Donnachie, P. V. Landshoff, Phys. Lett. B **478**, 146 (2000)
4. P.G.O. Freund, Nuovo Cimento A **48**, 541 (1967)
5. HERMES Collaboration, K. Ackerstaff et al., Eur. Phys. J. C **18**, 303 (2000)
6. K. Schilling et al., Nucl. Phys. B **61**, 397 (1970); K. Schilling, G. Wolf, Nucl. Phys. B **61**, 381 (1973)
7. H. Fraas, Ann. Phys. **87**, 417 (1974)
8. HERMES Collaboration, A. Airapetian et al., Eur. Phys. J. C **17**, 389 (2000)
9. H. Fraas, Nuclear Phys. B **113**, 532 (1976)
10. HERMES Collaboration, A. Airapetian et al., Phys. Lett. B **513**, 301 (2001)
11. A. Sokolov, I. Ternov, Sov. Phys. Doklady **8**, 1203 (1964)
12. D. P. Barber et al., Nucl. Instr. and Meth. A **329**, 79 (1993)
13. M. Beckmann et al., Nucl. Instr. and Meth. A **479**, 334 (2002)

14. HERMES Collaboration, K. Ackerstaff et al., Phys. Rev. Lett. **82**, 1164 (1999)
15. HERMES Collaboration, K. Ackerstaff et al., Nucl. Instr. and Meth. A **417**, 230 (1998)
16. H. Avakian et al., Nucl. Instr. and Meth. A **417**, 69 (1998)
17. N. Akopov at al., Nucl. Instr. and Meth. A **479**, 511 (2002)
18. T. Sjöstrand et al., Comput. Phys. Commun. **135**, 238 (2001)
19. T. Sjöstrand, Chr. Friberg, J. High Energy Phys. 0009 (2000) 010
20. K. Lipka, PhD thesis, Humboldt Universität zu Berlin, Germany (2002), DESY-THESIS 2002-018
21. P. Söding, Phys. Lett. **19**, 702 (1996)
22. M. Tytgat, PhD thesis, Universiteit Gent, Belgium (2001), DESY-THESIS 2001-018
23. G. L. Rakness, PhD thesis, University of Colorado, USA (2000)
24. U. Stösslein for the HERMES Collaboration, Proc. of SPIN 2000: 14th International Spin Physics Symposium, edited by K. Hatanaka et al., Osaka, Japan, AIP Conf. Proc. **570**, 387 (2001); C. Weiskopf, PhD thesis, Friedrich-Alexander-Universität Erlangen-Nürnberg (2002), DESY-THESIS 2002-039
25. N. I. Kochelev et al., Phys. Rev. D **61**, 094008 (2000); Y. Oh et al., Phys. Rev. D **62**, 017504 (2000); N. I. Kochelev et al., Phys. Rev. D **65**, 097504 (2002); N. I. Kochelev et al., arXiv:hep-ph/0211121, DESY 02-191, submitted to Phys. Rev. D
26. A. Tripet for the SMC Collaboration, Nucl. Phys. B **79** (Proc. Suppl.) (1999) 529
27. A. Titov et al., Phys. Rev. C **58**, 2429 (1998); Phys. Rev. C **60**, 035205 (1999); Y. Oh et al., Phys. Lett. B **462**, 23 (1999); private communications